**International Journal of Intelligent Communication and Computer Science**
**Vol. 1, No. 1, 2023, Pages 26-37.**

# Advancing 5G Wireless Transmission: Hybrid Non-Linear Companding for PAPR Reduction in FBMC-Based Systems

**Jagriti Kumari[1] and Balwinder Raj[1]**

**Research Paper**

[1]Department of ECE, National Institute of Technical Teachers Training and Research Chandigarh, INDIA
Email: jagritim23@gmail.com
Received: 11 Jan 2023, Revised: 13 Jun 2023, Accepted: 23 July 2023

**Abstract:**

The continuous growth of data demands in wireless communication has spurred ongoing research in search of better transmission mechanisms. As the next-generation wireless technology, 5G waveform technology has emerged as a promising candidate. Among the various techniques explored for 5G implementation, Filter Bank Multicarrier (FBMC) has shown potential as an effective choice for wireless transmission. However, like many other transmission techniques, FBMC suffers from the Peak-to-Average Power Ratio (PAPR) problem, which can lead to signal distortion and inefficiencies during transmission. In this work, we propose a novel hybrid non-linear companding scheme specifically designed for PAPR reduction in FBMC-based 5G wireless transmission. The proposed scheme can be easily integrated into the transmitter with minimal complexity, making it practical for real-world applications. The primary focus of this paper is to present the simulated results of our proposed hybrid PAPR reduction scheme and compare with the state-of-the-art methods.

**Keywords:** Watermarking, DCT, DWT, PSNR, UIQI and SSIM

## 1. Introduction:

The mobile communication revolution was triggered by the advent of multi-carrier transmission technology. Initially, Orthogonal Frequency Division Multiplexing (OFDM) was utilized for mobile communication, but over time, various new variants of OFDM have been developed. Despite these variations, all OFDM-based systems still rely on Inverse Fast Fourier Transform (IFFT) and Fast Fourier Transform (FFT) techniques. In OFDM, the total available bandwidth is divided into NFFT carriers to minimize the complexity of channel equalization [1]. To ensure proper symbol reception even in the presence of delay spread caused by multipath channels, a cyclic prefix (CP) is appended at the end of each OFDM symbol. However, this cyclic prefix introduces redundant data transmission, negatively impacting the spectral efficiency of the system. To address these limitations, FBMC systems have been introduced. FBMC (Filter Bank Multicarrier) employs carefully designed prototype filters to effectively mould the spectral characteristics of individual subcarriers, as well as the entire transmitted signal as a whole. In the context of FBMC, the choice of prototype filters is crucial in achieving superior spectral containment and minimizing interference between adjacent subcarriers. By utilizing well-shaped filters, FBMC ensure that each subcarrier's spectral footprint is precisely defined, resulting in reduced out-of-band emissions and enhanced spectral efficiency. By using nonrectangular pulse shapes and extending the duration of the prototype filters, FBMC achieves subcarriers with sharper frequency responses, reduced side lobes, and increased bandwidth efficiency. The absence of a cyclic prefix in most FBMC channels further enhances the spectral efficiency due to well-localized filters in the time and frequency domains. Despite the advantages of FBMC, it also faces the PAPR issue, similar to other FFT/IFFT-based wireless transmission techniques [2-4]. Addressing this issue often involves the implementation of high-power amplifiers endowed with a wide dynamic range.

In order to overcome the challenge at hand effectively, the deployment of high-power amplifiers boasting a high dynamic range has become a prevalent and practical solution. Companding techniques can be employed to reduce PAPR, but they may lead to a decrease in the system's Bit Error Rate (BER) performance [5]. In this

context, a new method is introduced for PAPR reduction in FBMC with the use of A-law and μ-law companding methods. This technique effectively decreases PAPR, although it results in an increased BER for the system. Our study reveals that both companding techniques yield comparable results as far as PAPR reduction is concerned, with Mu-law companding demonstrating slightly better performance. Shaeen et al. [6] evaluated numerous non-linear companding techniques for reducing PAPR in FBMC/OQAM systems while maintaining a decent Bit Error Rate. After an extensive analysis, it was concluded that Mu-law companding outperforms other techniques, providing superior PAPR reduction capabilities.

The mobile communication revolution owes much to multi-carrier transmission technology, with OFDM being a key player initially and various OFDM variants emerging later. However, the limitations of traditional OFDM, such as the use of a cyclic prefix and PAPR issues, have led to the exploration of FBMC as a more bandwidth-efficient alternative. Despite PAPR challenges in FBMC, our introduced A-law and μ-law companding techniques present effective solutions, with Mu-law showing particular promise for PAPR reduction in FBMC-based systems while maintaining acceptable BER performance. These advancements pave the way for more efficient and reliable wireless communication systems in the future.

## 2. PAPR reduction using Clipping and Non –linear Companding transform techniques

This section describes the clipping and non-linear companding schemes:

### A. Clipping of FBMC Sub-carriers

The clipping of sub carriers can be used to reduce PAPR. Considering the transmitted signal as $s(u)$, and its '$i^{th}$' sub carrier as $s^i(u)$ then we define clipping as under:

$$s_c^i(u) = \begin{cases} s^i(u) & \text{if } |s^i(u)| \le \gamma \\ \gamma & \text{if } |s^i(u)| > \gamma \end{cases} \quad (1)$$

where, γ is predefined clipping level. Therefore the clipped composite signal is given as

$$s_c(u) = \sum_{i=1}^{N} s_c^i(u) = \sum_{i=1}^{N} \begin{cases} s^i(u) & \text{if } |s^i(u)| \le \gamma \\ \gamma & \text{if } |s^i(u)| > \gamma \end{cases} \quad (2)$$

Further, calculating the power of the original and clipped signals, power of original signal is given by

$$p(u) = |s(u)|^2 \quad (3)$$

and the power of the clipped signal is given by

$$p_c(u) = |s_c(u)|^2 = \sum_{i=1}^{N} |s_c^i(u)|^2 = \sum_{i=1}^{N} \begin{cases} |s^i(u)|^2 & \text{if } |s^i(u)| \le \gamma \\ |\gamma|^2 & \text{if } |s^i(u)| > \gamma \end{cases} \quad (4)$$

It is noticeable that $p_c(u) < p(u)$. Therefore, clipping reduces SNR (Signal to noise ratio) and in turn increases BER. Therefore power restoration is necessary to avoid BER degradation.

### B. μ-Law Mapping

Companding methods proved to be quite effective in addressing the issue of amplitude variations in communication systems. These variations, known as the PAPR, can lead to undesirable effects such as distortion and interference during transmission. One widely used companding method is μ-law companding, also known as u-law companding, which is commonly employed in telecommunications and digital audio systems. The μ-law companding technique applies a non-linear transformation to the input signal, compressing its dynamic range and reducing the amplitude fluctuations. This compression is particularly beneficial in scenarios where the input signal exhibits a wide range of amplitudes, as it effectively redistributes the signal's power to reduce peaks. The companding process involves several steps: First, the absolute value of the input signal |s| is taken to eliminate the sign information temporarily. Then, the signal is multiplied by the companding parameter μ. The natural logarithm of (1+μ|s) is computed, followed by division by the logarithm of 1+μ. Finally, the sign of the original input signal is reintroduced to the result.

$$s_{\mu}^{i}(u) = \frac{\max(s(u))\ln\left(1+\frac{\mu\left|s^{i}(u)\right|}{\max(s(u))}\right)}{\ln(1+\mu)}\operatorname{sgn}(s^{i}(u)) \tag{5}$$

The original signal is restored at the receiver site using a μ-law expander as

$$s^{i}(u) = \frac{\max(s_{\mu}(u))}{\mu}\left(e^{\left|s_{\mu}^{i}(u)\right|\frac{\ln(1+\mu)}{\max(s_{\mu}(u))}}-1\right)\operatorname{sgn}(s_{\mu}^{i}(u)) \tag{6}$$

The power of the companded signal is given by

$$p_{\mu}(u) = \sum_{i=1}^{N}\left|s_{\mu}^{i}(u)\right|^{2} \tag{7}$$

The main idea is to maintain signal power of the original FBMC using μ Law companding which compensate for power loss due to the clipping of the sub carriers.

## 3. FBMC PAPR reduction using signals copies

Applying the Discrete Fourier Transform (DFT) to input symbols proves to be beneficial in various communication systems. It typically leads to a reduction in PAPR by introducing a single carrier effect. However, when dealing with FBMC systems, the presence of phasor terms prevents the observation of a single carrier effect. To address this limitation, Dongjun et al. [7] proposed a solution involving the inclusion of additional phasor terms, which effectively reduces PAPR. This condition is commonly referred to as the "ITSM" (Identically Time Shifted Multicarrier) condition [8]. The implementation details of the FBMC system, which incorporates the ITSM condition for PAPR reduction, are depicted in Figure 1.

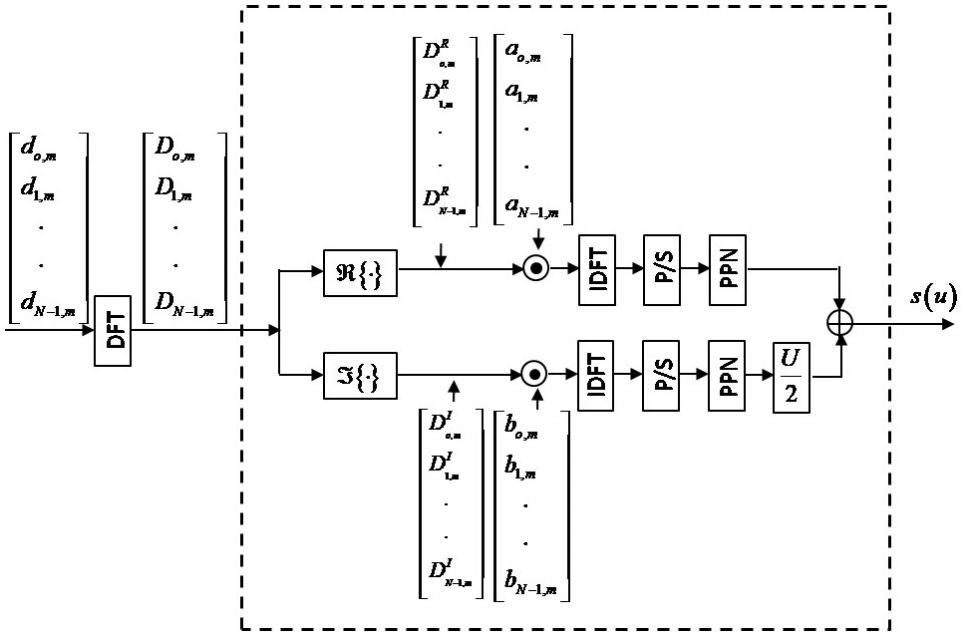


**Figure 1: Implementation of FBMC**

This figure illustrates the specific configuration and arrangement of the phasor terms and additional components within the FBMC system, highlighting how the ITSM condition is met to achieve improved PAPR performance. Overall, the use of DFT in combination with the ITSM condition presents a promising solution to improve the perforance3 and reliability of FBMC systems, particularly in scenarios where reducing PAPR is crucial for maintaining signal quality and spectral efficiency. Dongjun et al.'s [7] work contributes valuable

insights into optimizing multicarrier transmission techniques and addressing the challenges posed by PAPR in advanced communication systems.

Considering that the DFT of $d_{\alpha,\beta} = d^R_{\alpha,\beta} + jd^I_{\alpha,\beta}$ as $D_{\alpha,\beta} = D^R_{\alpha,\beta} + jD^I_{\alpha,\beta}$ as in FBMC OQAM modulation is considered, therefore in phase and quadrature components are π/2 shifted. Therefore, to achieve shift both real and imaginary components are first separated, and multiplied by $a_{\alpha,\beta}$ and $b_{\alpha,\beta}$ to achieve single carrier effect. The time domain signal is again obtained by taking IDFT, the time domain signal is then passes thorugh poly phase networks (PPN) which is nothing but series of filters and the quadrature components is π/2 shifted finally the both real and imaginary components are added to obtain signal $x(u)$ [7].

Referring Figure 1, $D^R_{\alpha,\beta}$ and $D^I_{\alpha,\beta}$ are element wise by multiplied by $a_{\beta,\alpha}$ and $b_{\beta,\alpha}$ respectively. In general $a_{\beta,\alpha}$ and $b_{\beta,\alpha}$ are expressed as

$$a_{\beta,\alpha} = j^{\beta+2\alpha}$$
$$b_{\beta,\alpha} = j^{\beta+2\alpha+1} \tag{8}$$

The transmitted signal's continuous version can be written as [7]

$$\begin{aligned} s(u) &= \sum_{\beta=0}^{N-1}\left\{\sum_{\alpha=0}^{M-1}(-1)^{\alpha}\, j^{\beta} D^R_{\alpha,\beta} F\left(u-\alpha U\right)\right\} e^{j\beta\frac{2\pi}{U}u} \\ &\quad + \sum_{\beta=0}^{N-1}\left\{\sum_{\alpha=0}^{M-1}(-1)^{\alpha}\, j^{\beta+1} D^I_{\alpha,\beta} F\left(u-\alpha U-\frac{U}{2}\right)\right\} e^{j\beta\frac{2\pi}{U}\left(u-\frac{U}{2}\right)} \qquad (9) \\ &= \sum_{\beta=0}^{N-1}\sum_{\alpha=0}^{M-1}(-1)^{\alpha}\left\{D^R_{\alpha,\beta} F\left(u-\alpha U\right) e^{j\beta\frac{2\pi}{U}\left(u+\frac{U}{4}\right)} + jD^I_{\alpha,\beta} F\left(u-\alpha U-\frac{U}{2}\right) e^{j\beta\frac{2\pi}{U}\left(u+\frac{U}{4}-\frac{U}{2}\right)}\right\} \end{aligned}$$

In the given example, the variable "M" represents the number of Offset Quadrature Amplitude Modulation (OQAM) symbols present in each carrier within a single frame. For the sake of simplicity, we will consider that the pulse shape function, denoted as "F(u)," is equal to 1 and that its duration is represented by "T." Consequently, the overlap interval for the m-th carrier can be expressed as ( $\alpha$ $U$ + $U$/2) ≤ u ≤ ( $\alpha$ +1)$U$. By transforming the equation provided above, we can further elaborate on the relationship between the time index "u" and the carrier index " $\alpha$ ".

For the $\alpha$ th carrier, the start of the overlap interval is given by " $\alpha$ $U$ + $U$/2," and the end of the overlap interval is represented by "( $\alpha$ +1)$U$." This indicates that the carrier signals within each frame overlap with their neighbouring carriers over a specific time duration. In OQAM systems, the overlapping nature of the carriers is a key feature that allows for effective interference management and improved spectral efficiency. The unique characteristics of OQAM modulation enable it to mitigate the effects of intersymbol interference and maintain orthogonality among the carriers, even in scenarios with severe channel conditions.

$$s(u) = (-1)^{\alpha}\left\{\sum_{\beta=0}^{N-1} D^R_{\alpha,\beta} e^{j\beta\frac{2\pi}{U}\left(u+\frac{U}{4}\right)} + j\sum_{\beta=0}^{N-1} D^I_{\alpha,\beta} e^{j\beta\frac{2\pi}{U}\left(u+\frac{U}{4}-\frac{U}{2}\right)}\right\} \tag{10}$$

Moreover we have

$$D_{\beta,\alpha} = \sum_{k=0}^{N-1} d_{k,\alpha} e^{-j\frac{2\pi}{N}\beta k}\,. \tag{11}$$

Further we have

$$D^R_{\alpha,\beta} = \frac{D_{\beta,\alpha} + D^*_{\beta,\alpha}}{2} \text{ and } D^I_{\alpha,\beta} = \frac{D_{\beta,\alpha} - D^*_{\beta,\alpha}}{2j}\,. \tag{12}$$

Equation 10 can be written as [8]

$$s(u)=\frac{(-1)^{\alpha}}{2}\left(\sum_{\beta=0}^{N-1}D_{\beta,\alpha}e^{j\beta\frac{2\pi}{U}\left(u+\frac{U}{4}\right)}+\sum_{\beta=0}^{N-1}D^{*}{}_{\beta,\alpha}e^{j\beta\frac{2\pi}{U}\left(u+\frac{U}{4}\right)}\right.$$
$$\left.+\sum_{\beta=0}^{N-1}D_{\beta,\alpha}e^{j\beta\frac{2\pi}{T}\left(u+\frac{U}{4}-\frac{U}{2}\right)}-\sum_{\beta=0}^{N-1}D^{*}{}_{\beta,\alpha}e^{j\beta\frac{2\pi}{U}\left(u+\frac{U}{4}-\frac{U}{2}\right)}\right) \tag{13}$$

Expanding first term only,

$$\sum_{\beta=0}^{N-1}D_{\beta,\alpha}e^{j\beta\frac{2\pi}{U}\left(u+\frac{U}{4}\right)}=\sum_{\beta=0}^{N-1}\left(\sum_{k=0}^{N-1}d_{k,\alpha}e^{-j\frac{2\pi}{N}\beta k}\right)e^{j\beta\frac{2\pi}{U}\left(u+\frac{U}{4}\right)}=\sum_{k=0}^{N-1}d_{k,\alpha}\sum_{\beta=0}^{N-1}e^{j\frac{2\pi\beta}{U}\left(u-\frac{U}{N}k+\frac{U}{4}\right)}$$
$$=\sum_{k=0}^{N-1}d_{k,\alpha}u\left(u-\frac{U}{N}k+\frac{U}{4}\right) \tag{14}$$

where,

$$\upsilon(u)=\sum_{\beta=0}^{N-1}e^{j\frac{2\pi\beta}{U}u}=\frac{\sin\left(\frac{\pi N}{U}u\right)}{\sin\left(\frac{\pi}{U}u\right)}e^{j\frac{(N-1)\pi}{U}u}.$$

or

$$\left|\upsilon(u)\right|=\frac{\sin\left(\frac{\pi N}{U}u\right)}{\sin\left(\frac{\pi}{U}u\right)}. \tag{15}$$

Equation 15, represents a sinc pulse i.e., single carrier effect. Again considering equation 14, in this equation, a time shift of U/4 occurs between the data symbol and the pulse train. By cyclically shifting the data symbols, the overall time shift is reduced to zero.

$$\sum_{k=0}^{N-1}d_{k,\alpha}f\left(u-\frac{U}{N}k+\frac{U}{4}\right)=\sum_{k=0}^{N-1}d_{k,\alpha}f\left(u-\frac{U}{N}\left(k-\frac{N}{4}\right)\right)=\sum_{k=0}^{N-1}d_{\left[\left(k+\frac{N}{4}\right)\bmod N\right],\alpha}f\left(u-\frac{U}{N}k\right). \tag{16}$$

Similarly writing other terms equation 15 can be written as

$$s(u)=\frac{(-1)^{\alpha}}{2}\left(\sum_{k=0}^{N-1}d_{\left[\left(k+\frac{N}{4}\right)\bmod N\right],\alpha}+\sum_{\beta=0}^{N-1}d^{*}{}_{\left[\left(\frac{3N}{4}-k\right)\bmod N\right],\alpha}\right.$$
$$\left.+d_{\left[\left(k-\frac{N}{4}\right)\bmod N\right],\alpha}-d^{*}{}_{\left[\left(\frac{5N}{4}-k\right)\bmod N\right],\alpha}\right)\upsilon\left(u-\frac{U}{N}k\right) \tag{17}$$

As a result, four data symbols are added in parallel in a single carrier. As a result, a decrease in PAPR can be predicted when compared to FBMC without spread.

**A. Phase shift condition for each carrier (ITSM)**

Re-writing equation 10 as:

$$s(u)=(-1)^{\alpha}\left\{\sum_{\beta=0}^{N-1}D_{\alpha,\beta}^{R}+j(-1)^{\beta}D_{\alpha,\beta}^{I}\right\}e^{j\beta\frac{2\pi}{U}\left(u+\frac{U}{4}\right)} \tag{18}$$

s($u$) will become a single carrier pure sinusoid if $(-1)^{\beta} D^{I}_{\alpha,\beta}$ term is positive and can be done in two ways i.e., by multiplying $(-1)^{\beta}$ to $(-1)^{\beta} D^{I}_{\alpha,\beta}$ or multiplying $(-1)^{\beta}$ to $(-1)^{\alpha} j^{\beta+1}$. This condition is known as ITSM [13].

Finally, taking into account the filter response $F(u)$, the transmitted signal in a generalized form can be defined as:

$$s(u)=\sum_{\beta=0}^{N-1}\sum_{\alpha=0}^{M-1}(-1)^{\alpha}\left\{D^{R}_{\alpha,\beta}F\left(u-\alpha U\right)+j\,D^{I}_{\alpha,\beta}F\left(u-\alpha U-\frac{U}{2}\right)\right\}e^{j\beta\frac{2\pi}{U}\left(u+\frac{U}{4}\right)} \tag{19}$$

Since the phase shifting sign has an effect on the effects, s(t) can also be written as

$$s(u)=\sum_{\beta=0}^{N-1}\sum_{\alpha=0}^{M-1}(-1)^{\alpha}\left\{D^{R}_{\alpha,\beta}F\left(u-\alpha U\right)+j\,D^{I}_{\alpha,\beta}F\left(u-\alpha U-\frac{U}{2}\right)\right\}e^{j\beta\frac{2\pi}{U}\left(u-\frac{U}{4}\right)} \tag{20}$$

We build data frames using these two types of continuous time signals. In each block of the data frame, there are 'v' FBMC symbols. Considering ($p$+1)$^{th}$ frame then we have

$$s_p^{(1)}(u)=\sum_{\beta=0}^{N-1}\sum_{\alpha=pv}^{(p+1)v-1}(-1)^{\alpha}\left\{D^{R}_{\alpha,\beta}F\left(u-\alpha U\right)+jD^{I}_{\alpha,\beta}F\left(u-\alpha U-\frac{U}{2}\right)\right\}e^{j\beta\frac{2\pi}{U}\left(u+\frac{U}{4}\right)} \tag{21}$$

$$s_p^{(2)}(u)=\sum_{\beta=0}^{N-1}\sum_{\alpha=pv}^{(p+1)v-1}(-1)^{\alpha}\left\{D^{R}_{\alpha,\beta}F\left(u-\alpha U\right)+jD^{I}_{\alpha,\beta}F\left(u-\alpha U-\frac{U}{2}\right)\right\}e^{j\beta\frac{2\pi}{U}\left(u-\frac{U}{4}\right)} \tag{22}$$

By altering the delay from imaginary to real part, the signals remain unaffected, resulting in the following:

$$s_p^{(3)}(u)=\sum_{\beta=0}^{N-1}\sum_{\alpha=pv}^{(p+1)v-1}(-1)^{\alpha}\left\{D^{R}_{\alpha,\beta}F\left(u-\alpha U-\frac{U}{2}\right)+jD^{I}_{\alpha,\beta}F\left(u-\alpha U\right)\right\}e^{j\beta\frac{2\pi}{U}\left(u+\frac{U}{4}\right)} \tag{23}$$

$$s_p^{(4)}(u)=\sum_{\beta=0}^{N-1}\sum_{\alpha=pv}^{(p+1)v-1}(-1)^{\alpha}\left\{D^{R}_{\alpha,\beta}F\left(u-\alpha U-\frac{U}{2}\right)+jD^{I}_{\alpha,\beta}F\left(u-\alpha U\right)\right\}e^{j\beta\frac{2\pi}{U}\left(u-\frac{U}{4}\right)} \tag{24}$$

Multiplying $s_p^{(3)}(t)$ and $s_p^{(4)}(t)$ by $j$ to make them equivalent to $s_p^{(1)}(t)$ and $s_p^{(2)}(t)$ to obtain

$$s_p^{(3)}(u)=\sum_{\beta=0}^{N-1}\sum_{\alpha=pv}^{(p+1)v-1}(-1)^{\alpha}\left\{jD^{R}_{\alpha,\beta}F\left(u-\alpha U-\frac{U}{2}\right)-D^{I}_{\alpha,\beta}F\left(u-\alpha U\right)\right\}e^{j\beta\frac{2\pi}{U}\left(u+\frac{U}{4}\right)} \tag{25}$$

$$s_p^{(4)}(u)=\sum_{\beta=0}^{N-1}\sum_{\alpha=pv}^{(p+1)v-1}(-1)^{\alpha}\left\{jD^{R}_{\alpha,\beta}F\left(u-\alpha U-\frac{U}{2}\right)-D^{I}_{\alpha,\beta}F\left(u-\alpha U\right)\right\}e^{j\beta\frac{2\pi}{U}\left(u-\frac{U}{4}\right)} \tag{26}$$

The signal with the minimum peak power is initially selected from the first block (p=0), and subsequently, successive candidates are combined to create blocks. Let $bl_p(t)$ denote the concatenated waveform up to the $p^{h}$ block, then we have:

$$bl_p(u)=bl_{p-1}(u)+s_p^{(k_u)}(u),\quad with\ bl_{p-1}(u)=0 \tag{27}$$

$$k_l=\begin{cases}\underset{z\in\{1,2,3,4\}}{\arg\min}\left\{\max_{u\in R}\left|s_p^{(z)}(u)\right|^2\right\}, & if\ \ p=0\\ \underset{z\in\{1,2,3,4\}}{\arg\min}\left\{\max_{u\in R}\left|bl_{p-1}(u)\ +s_p^{(z)}(u)\right|^2\right\}, & else\end{cases} \tag{28}$$

**B. PAPR reduction**

The clipping rule is defined as

$$\overline{s}_p(u)=\begin{cases} s_p(u) & \text{if } |s_p(u)|\le A_{Cl} \\ A_C e^{j\phi[s(u)]} & \text{if } |s_p(u)|> A_{Cl} \end{cases} \tag{29}$$

The block equation modifies to

$$cl_p(u)=cl_{p-1}(u)+\overline{s}_p^{(k_u)}(u),\quad with\ cl_{p-1}(u)=0 \tag{30}$$

$$k_l=\begin{cases} \arg\min\limits_{z\in\{1,2,3,4\}}\left\{\max\limits_{u\in R}\left|\overline{s}_p^{(z)}(u)\right|^2\right\}, & if\ \ p=0 \\ \arg\min\limits_{z\in\{1,2,3,4\}}\left\{\max\limits_{u\in R}\left|cl_{p-1}(u)\ +\overline{s}_p^{(z)}(u)\right|^2\right\}, & else \end{cases} \tag{31}$$

Non-linear companding techniques can further minimize variations in a selected block. It has recently been demonstrated that μ-Law companding is an effective technique for lowering PAPR in traditional FBMC-OQAM. As shown in equation, 31, we used μ-Law companding on the chosen block (30). The signal is compressed using [9-13]

$$s_{p\mu_c}(u)=\frac{\max(\overline{s}_p(u))\ln\left(1+\dfrac{\mu_c\overline{s}_p(u)}{\max(\overline{s}_p(u))}\right)}{\ln(1+\mu_c)}\operatorname{sgn}(\overline{s}_p(u)) \tag{32}$$

The below given equation restore the companded signal to original signal:

$$\overline{s}_p(u)=\frac{\max(s_{p\mu_c}(u))}{\mu_c}\left(e^{\left|\overline{x}_{c\mu_c}(u)\right|\frac{\ln(1+\mu_c)}{\max(s_{p\mu_c}(u))}}-1\right)\operatorname{sgn}(s_{p\mu_c}(u)) \tag{33}$$

The block equation modifies to

$$cl_{\mu_c p}(u)=cl_{\mu_c p-1}(u)+s_{p\mu_c}^{(k_u)}(u),\quad with\ cl_{\mu_c p-1}(u)=0 \tag{34}$$

$$k_l=\begin{cases} \arg\min\limits_{z\in\{1,2,3,4\}}\left\{\max\limits_{u\in R}\left|s_{p\mu_c}^{(z)}(u)\right|^2\right\}, & if\ \ p=0 \\ \arg\min\limits_{z\in\{1,2,3,4\}}\left\{\max\limits_{u\in R}\left|cl_{\mu_c p-1}(u)\ +s_{p\mu_c}^{(z)}(u)\right|^2\right\}, & else \end{cases}$$

The PAPR of final companded FBMC signal is obtained as

$$PAPR=\frac{\max_{(\alpha-1)U<u<\alpha U}\left|s_{p\mu_c}^{(k_t)}(u)\right|^2}{E\left[\left|s_{p\mu_c}^{(k_u)}(u)\right|^2\right]},\alpha=0,1.....M-1 \tag{35}$$

## 4. Simulation Results using MATLAB

Here, the simulated results of our novel hybrid PAPR reduction scheme are expained. To conduct the simulations, we have set up a simulation environment using the mathematical description provided in the previous chapter. Within this environment, we explore the effectiveness of our proposed technique in reducing the PAPR of the transmitted signal. Firstly, we determine the optimal clipping levels and the value of μ for our scheme, aiming to minimize the Complementary Cumulative Distribution Function (CCDF). This step is crucial in achieving a significant reduction in PAPR while maintaining the overall signal quality. Next, we examine the signal variations at different stages of our proposed method. By plotting these variations, we gain insights into how the signal is processed and how the PAPR reduction is achieved through our hybrid companding scheme. Furthermore, we analyze the results of the CCDF versus PAPR. This analysis provides a

comprehensive view of the trade-off between PAPR reduction and signal performance, allowing us to assess the overall effectiveness of our approach. Finally, we compare the results obtained from our proposed hybrid PAPR reduction scheme with those from other recently proposed notable PAPR reduction techniques. This comparative analysis gives us a clear understanding of how our approach fares against state-of-the-art methods in terms of PAPR reduction and signal quality.

**Table 1: List of important simulation parameters**

| Parameter | Value |
|---|---|
| Number of subcarriers | 64 |
| Number of FBMC symbols per frame | 48 |
| Overlapping factor | 4 |
| Clipping level | 0.7×signal peak power |
| Number of frames for PAPR check | 1000 |

In figure 2, block addition is shown. Using mathematical details as above (eqn. 27), four copies of signal is created, and PAPR of each block is evaluated and block with min PAPR is selected, similarly in the next block same process is repeated and again block with min PAPR is selected, and finally two min blocks are combined together.

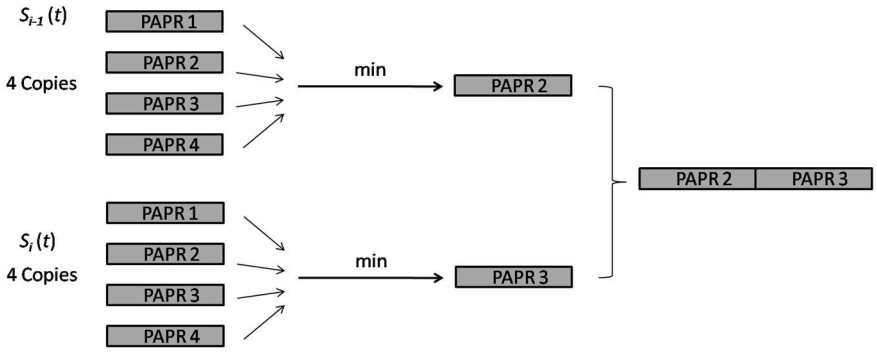


**Figure 2: Schematic of block addition**

Using parameters given in Table 1, the PAPR of four copies of a signal is shown in figure with PAPRs values as 90, 4.62, 5.12 and 4.02 dB. Out of these four copies one with minimum will be selected.

PAPR =min [PAPR1, PAPR2, PAPR3, PAPR4]

PAPR =min [3.90 4.62 5.12 4.02] = 3.90

PAPR =min [5.68 3.79 4.42 4.37] = 3.79

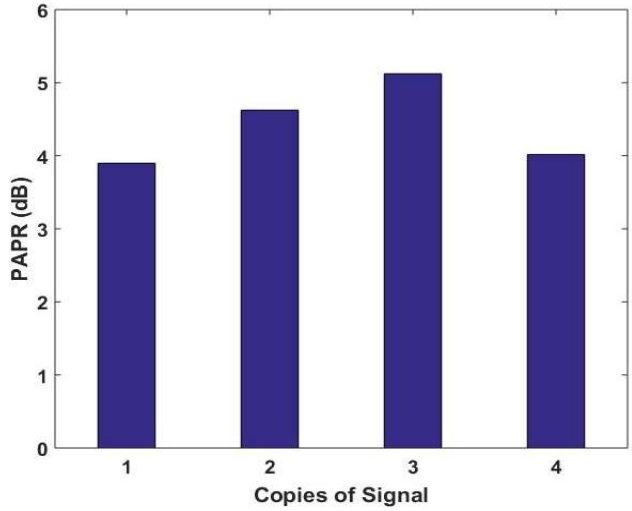


**Figure 3: PAPR of 4 copies of signal (instant *i*-1)**

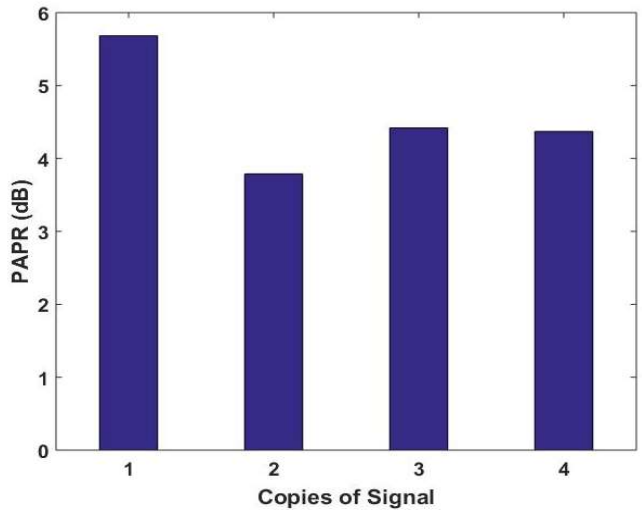


**Figure 4: PAPR of 4 copies of signal (instant *i*)**

Therefore copy 1 from instant (*i*-1) and copy 2 from instant (*i*) will be selected to form block. In figure 5, transmitted FBMC signal is shown, here maximum amplitude is 0.04383 and minimum value of amplitude is -0.04238. The fluctuation in the amplitudes is significant and leads to the PAPR. The variation in the amplitude arises due to two factors i.e., IDFT and frequency response of the filters.

To suppress large values of the amplitude next clipping is applied while considering $A_{cl}$= 0.7 max [$s(u)$], this condition reduces the values of the larger peak, still variation in the amplitude is significant and can be observed (Figure 5).

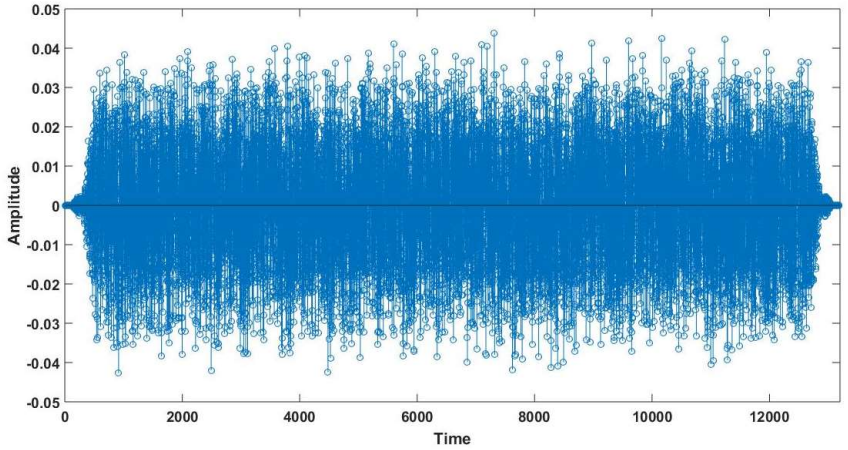


**Figure 5: Transmitted FBMC signal**

To further reduce amplitude variations we applied μ Law on the clipped signal, here it can be seen that the amplitude fluctuations have been reduced considerably (Figure 6). In the experiment carried out the power of original signal is 2.281 $\times 10^{-4}$ units. The power of the clipped signal is 1.61 $\times 10^{-4}$ units, and finally power after applying μ law companding and second level of clipping with clipping level as $A_{cl}$= 0.6 max [companded $s(u)$] is 2.285 $\times 10^{-4}$ units.

Figure 7 illustrates the CCDF plotted against the PAPR for various latest PAPR reduction mechanisms applied in FBMC systems. The results are analyzed at a CCDF level of $10^{-3}$, while the x-axis represents the PAPR denoted by "X" in dB. In Table 1, the fundamental parameters considered for these simulations are provided. The conventional FBMC technique yields a PAPR value of 11 dB. By incorporating DFT-based spreading in FBMC, the PAPR is reduced to 9 dB [15]. Employing Partial Transmit Sequence (PTS) for PAPR reduction with conventional FBMC further decreases the PAPR to 8 dB [16], and with Tone Reservation (TR) technique, it is reduced to 7.6 dB [17], while including the ITSM condition along with DFT in FBMC leads to a PAPR of 7.1 dB.

The hybrid method introduced very recently, which combines Multi Data Block PTS along with TR (MDB-PTS + TR) the obtained PAPR, is 7 dB [18]. By incorporating μ-law companding on conventional FBMC, the PAPR is further reduced to 6.5 dB [6]. Introducing the advanced PTS (M-PTS) scheme yields a PAPR of 6.2 dB [19]. With our proposed hybrid nonlinear companding scheme, the PAPR reaches an impressively low value of 2.1 dB. These results clearly demonstrate the effectiveness of our novel hybrid PAPR reduction scheme in significantly mitigating PAPR in FBMC systems compared to other existing techniques. The reduction in PAPR achieved by our proposed scheme is essential for enhancing the spectral efficiency and overall performance of next-generation wireless transmission technologies.

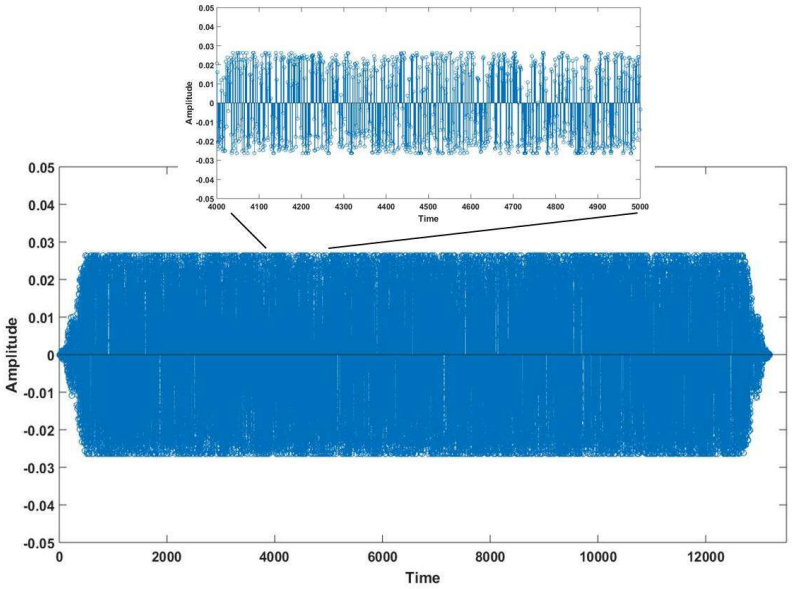


**Figure 6: Clipped and companded FBMC signal**

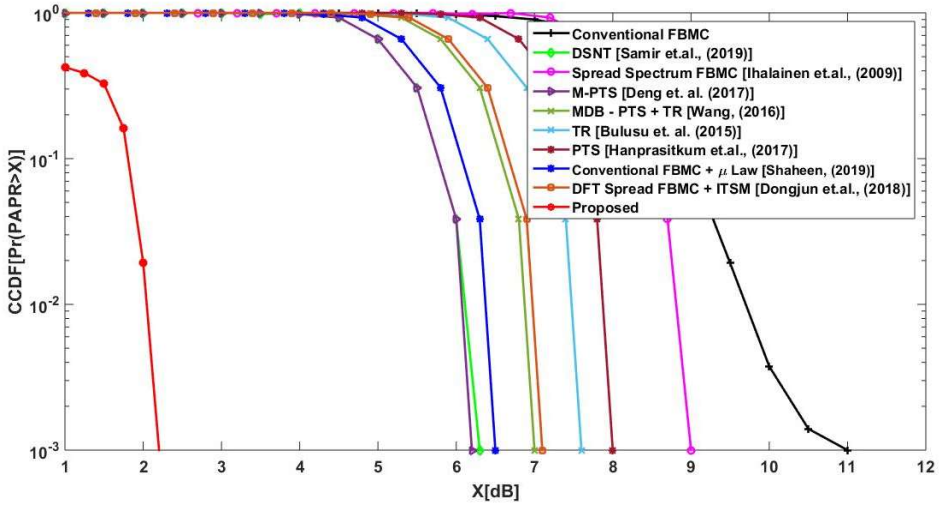


**Figure 7: Companded and clipped FBMC signal**

## 5. Conclusions

This paper focuses on the FBMC scheme and aims to classify it through mathematical modelling. The discussion begins by exploring the concept of single carrier effect and deriving the ITSM conditions, which play a crucial role in FBMC systems. Additionally, the paper delves into block concatenation, a key technique used for PAPR reduction in FBMC. Two specific methods for PAPR reduction are thoroughly examined: clipping and μ-law companding schemes. An analysis of past PAPR reduction schemes reveals that most of them yield a PAPR value of around 7.0 dB. The introduction of the μ-law companding scheme, although simple to implement, brings the PAPR down to approximately 6.5 dB. However, the proposed hybrid non-

linear companding scheme surpasses all other techniques, yielding an impressively low PAPR value of only 2.1 dB. These findings emphasize the superiority of the proposed hybrid non-linear companding scheme over existing methods, making it a highly promising approach for enhancing the efficiency and performance of FBMC-based wireless communication systems. The significant reduction in PAPR achieved by this scheme contributes to better spectral efficiency and overall system reliability, which are essential factors for advancing next-generation wireless communication technologies.

**References**


[1] C. Ye, Z. Li, T. Jiang, C. Ni, and Q. Qi, ''PAPR reduction of OQAM-OFDM signals using segmental PTS scheme with low complexity,'' *IEEE Trans. Broadcast.*, Vol. 60, No. 1, pp. 141–147, Mar. 2014.

[2] H. Wang, "A hybrid PAPR reduction method based on SLM and multi-data block PTS for FBMC/OQAM systems" Information, Vol. 9, No.10, p.246, 2018.

[3] Yang, Y., & Xu, P., "PAPR Reduction of FBMC-OQAM Signals Using Particle Swam Optimization Algorithm Based on MBJO-PTS" In International Conference on Intelligent and Interactive Systems and Applications (pp. 167-176). Springer, Cham, 2018.

[4] Agarwal, A., & Sharma, R, "Review of Different PAPR Reduction Techniques in FBMC-OQAM System" In Internet of Things and Big Data Applications (pp. 183-191). Springer, Cham, 2020

[5] Hasan, Abdullah, Muhammad Zeeshan, Muhammad Ali Mumtaz, and Muhammad Waqas Khan. "PAPR reduction of FBMC-OQAM using A-law and Mu-law companding." In *2018 ELEKTRO*, pp. 1-4. IEEE, 2018.

[6] Shaheen, Imad A., AbdelhalimZekry, Fatma Newagy, and Reem Ibrahim. "Performance evaluation of PAPR reduction in FBMC system using Nonlinear companding transform." ICT Express, Vol. 5, No. 1, pp.41-46, 2019.

[7] Na, Dongjun, and Kwonhue Choi. "Low papr fbmc." IEEE Transactions on Wireless Communications, Vol. 17, No. 1, pp.182-193, 2017.

[8] Srivastava, Mohit Kumar, Manoj Kumar Shukla, Neelam Srivastava, and Ashok Kumar Shankhwar. "A Hybrid Scheme for Low PAPR in Filter Bank Multi Carrier Modulation." *Wireless Personal Communications* 113, no. 2 (2020): 1009-1028.

[9] Shiv Om Tiwari, Rajeev Paulus. "Non-linear companding scheme for peak-to-average power ratio (PAPR) reduction in generalized frequency ivision multiplexing", Journal of Optical Communications, 2020.

[10] Hasan, Abdullah, Muhammad Zeeshan, Muhammad Ali Mumtaz, and Muhammad Waqas Khan. "PAPR reduction of FBMC-OQAM using A-law and Mu-law companding." In *2018 ELEKTRO*, pp. 1-4. IEEE, 2018.

[11] Ramavath, Srinivas, and Umesh Chandra Samal. "Theoretical Analysis of PAPR Companding Techniques for FBMC Systems." *Wireless Personal Communications* (2021): 1-17.

[12] Agarwal, A., & Sharma, R. (2020). Review of different PAPR reduction techniques in FBMC-OQAM system. In *Internet of Things and Big Data Applications* (pp. 183-191). Springer, Cham.

[13] Xi, Siyu, Zhangdui Zhong, Yinsheng Liu, Xia Chen, Fanggang Wang, and Deshan Miao. "DFT-spread universal filtered multi-carrier for 5G." In *2016 2nd IEEE International Conference on Computer and Communications (ICCC)*, pp. 1591-1596. IEEE, 2016.

[14] Ikni, S., Abed, D., Redadaa, S., & Sedraoui, M. (2019). PAPR reduction in FBMC-OQAM systems based on discrete sliding norm transform technique. *Radioelectronics and Communications Systems,62*(2), 51–60.

[15] Ihalainen, T., Viholainen, A., Stitz, T. H., Renfors, M., & Bellanger, M. (2009). Filter bank based multi-mode multiple access scheme for wireless uplink. In *Proceedings European Signal Processing Conference,* August 2009, pp. 1354–1358.

[16] Deng, Honggui, Shuang Ren, Yan Liu, and Chengying Tang. "Modified PTS-based PAPR reduction for FBMC-OQAM systems." In *Journal of Physics: Conference Series*, vol. 910, no. 1, p. 012057. IOP Publishing, 2017.

[17] Bulusu, S. S. K. C., Shaiek, H., Roviras, D. (2015). Reduction of PAPR of FBMC-OQAM systems by dispersive tone reservation technique. In *Proceeding of International Symposium on Wireless Communication Systems*, 25–28 August 2015, Brussels, Belgium. IEEE.

[18] Wang, H., Wang, X., Xu, L., & Du, W. (2016). Hybrid PAPR reduction scheme for FBMC/OQAM systems based on multi data block PTS and TR methods. *IEEE Access,4*, 4761.

[19] Shi, Nan, and Shouming Wei. "A partial transmit sequences based approach for the reduction of peak-to-average power ratio in FBMC system." In 2016 25th Wireless and Optical Communication Conference (WOCC), pp. 1-3. IEEE, 2016.